

See discussions, stats, and author profiles for this publication at: <https://www.researchgate.net/publication/328011776>

# Effect of Iron Limitation on the Isotopic Composition of Cellular and Released Fixed Nitrogen in *Azotobacter vinelandii*

Article in *Geochimica et Cosmochimica Acta* - October 2018

DOI: 10.1016/j.gca.2018.09.023

CITATIONS

0

READS

33

8 authors, including:



Darcy L. McRose

California Institute of Technology

16 PUBLICATIONS 311 CITATIONS

[SEE PROFILE](#)



Oliver Baars

North Carolina State University

30 PUBLICATIONS 296 CITATIONS

[SEE PROFILE](#)



# Effect of iron limitation on the isotopic composition of cellular and released fixed nitrogen in *Azotobacter vinelandii*

D.L. McRose<sup>a,\*</sup>, A. Lee<sup>b</sup>, S.H. Kopf<sup>a,1</sup>, O. Baars<sup>a,2</sup>, A.M.L. Kraepiel<sup>c</sup>  
D.M. Sigman<sup>a</sup>, F.M.M. Morel<sup>a</sup>, X. Zhang<sup>a,d,\*</sup>

<sup>a</sup> Department of Geosciences, Princeton University, Princeton, NJ, USA

<sup>b</sup> Department of Ecology and Evolutionary Biology, Princeton University, Princeton, NJ, USA

<sup>c</sup> Department of Chemistry, Princeton University, Princeton, NJ, USA

<sup>d</sup> Princeton Environmental Institute, Princeton University, Princeton, NJ, USA

Received 11 April 2018; accepted in revised form 22 September 2018; Available online 1 October 2018

## Abstract

Most biological nitrogen transformations have characteristic kinetic isotope effects used to track these processes in modern and past environments. The isotopic fractionation associated with nitrogen fixation, the only biological source of fixed nitrogen (N), provides a particularly important constraint for studies of nitrogen cycling. Nitrogen fixation using the ‘canonical’ Mo-nitrogenase produces biomass with a  $\delta^{15}\text{N}$  value of ca.  $-1\text{‰}$  (vs. atmospheric  $\text{N}_2$ ). If the ‘alternative’ V- and Fe-only nitrogenases are used, biomass  $\delta^{15}\text{N}$  can be between  $-6\text{‰}$  and  $-7\text{‰}$ . These biomass values are assumed to be relatively invariant and to reflect the cellular level expressed isotope effect of nitrogen fixation. However, field and laboratory studies report wide ranges of diazotrophic biomass  $\delta^{15}\text{N}$  (from  $-3.6\text{‰}$  to  $+0.5\text{‰}$  for Mo-based nitrogen fixation). This variation could be partly explained by the release of dissolved organic N (DON) that is isotopically distinct from biomass. The model nitrogen fixer *Azotobacter vinelandii* secretes siderophores, small molecules that aid in Fe uptake and can comprise  $>30\%$  of fixed nitrogen. To test whether siderophores (and other released N) can decouple biomass  $\delta^{15}\text{N}$  from the isotope effect of nitrogen fixation we measured the isotopic composition of biomass and released N in Fe-limited *A. vinelandii* cultures fixing nitrogen with Mo- and V-nitrogenases. We report that biomass  $\delta^{15}\text{N}$  was elevated under Fe limitation with a maximum value of  $+1.2\text{‰}$  for Mo-based nitrogen fixation. Regardless of the nitrogenase isozyme used, released nitrogen  $\delta^{15}\text{N}$  was also  $2\text{--}3\text{‰}$  lower than biomass  $\delta^{15}\text{N}$ . Siderophore nitrogen was found to have a slightly higher  $\delta^{15}\text{N}$  than the rest of the DON pool but was still produced in large enough concentrations to account for increases in biomass  $\delta^{15}\text{N}$ . The low  $\delta^{15}\text{N}$  of siderophores (relative to biomass) is consistent with what is known from compound specific isotope studies of the amino acids used in siderophore biosynthesis, and indicates that other amino-acid derived siderophores should also have a low  $\delta^{15}\text{N}$ . The implications for studies of nitrogen fixation are discussed.

© 2018 Elsevier Ltd. All rights reserved.

**Keywords:** Nitrogen isotopes; Nitrogen fixation; Alternative nitrogenase; Iron; Kinetic isotope effect; Siderophore; *Azotobacter vinelandii*

\* Corresponding authors at: Division of Geological and Planetary Sciences, California Institute of Technology, Pasadena, California, USA and Division of Biology and Biological Engineering, California Institute of Technology, Pasadena, California, USA (D.L. McRose).

E-mail addresses: [mcrose@princeton.edu](mailto:mcrose@princeton.edu) (D.L. McRose), [xinningz@princeton.edu](mailto:xinningz@princeton.edu) (X. Zhang).

<sup>1</sup> Present Address: Department of Geological Sciences, University of Colorado, Boulder, CO, USA.

<sup>2</sup> Present Address: Department of Entomology and Plant Pathology, North Carolina State University, Raleigh, NC, USA.

## 1. INTRODUCTION

The isotopic fractionation associated with microbial nitrogen transformations can provide important biogeochemical insights (Brandes and Devol, 2002; Gruber and Galloway, 2008; Sigman et al., 2009a). Nitrogen fixation, the primary natural source of biologically available (‘fixed’) nitrogen is catalyzed by the metalloenzyme nitrogenase, which uses iron (Fe) in addition to molybdenum (Mo) or vanadium (V) to reduce  $N_2$  gas to  $NH_4^+$  (Bishop et al., 1986; Robson et al., 1986; Seefeldt et al., 2009). The bulk of newly fixed  $NH_4^+$  is converted to biomass and as a result, isotopic measurements of nitrogen fixer biomass ( $\delta^{15}N_{bio}$ ) are generally interpreted to directly reflect the cellular-level expressed kinetic isotope effect of nitrogen fixation, functionally defined hereafter as  $\epsilon_{Nfix} = \delta^{15}N_{aq} - \delta^{15}N_{bio}$ , where  $\delta^{15}N = [(^{15}N/^{14}N_{sample}) / (^{15}N/^{14}N_{air}) - 1] \times 1000$  and dissolved  $N_2$  ( $\delta^{15}N_{aq}$ ) =  $\sim +0.7\text{‰}$  (Klotts and Benson, 1963). Pure culture studies have shown that the isotope effect of nitrogen fixation is small (Hoering and Ford, 1960; Macko et al., 1987), leading to diazotrophic biomass  $\delta^{15}N$  measurements close to 0‰. Researchers often adopt a  $\delta^{15}N$  value of ca.  $-1\text{‰}$  for biomass produced by organisms using the ‘canonical’ Mo-nitrogenase (Brandes and Devol, 2002; Montoya, 2008; Sigman et al., 2009b). When ‘alternative’ V- or Fe-only nitrogenase isozymes are used, this value is much lower (ca.  $-6$  to  $-7\text{‰}$ , Rowell et al., 1998; Zhang et al., 2014). Fe limitation has been shown to increase the  $\delta^{15}N$  of biomass in the cyanobacterium *Anabaena variabilis* (Zerkle et al., 2008), whereas variations in carbon source, growth phase, nitrogenase activity, as well as the availability of molybdenum and phosphate have not been found to have an effect on biomass  $\delta^{15}N$  (Beaumont et al., 2000; Zerkle et al., 2008; Zhang et al., 2014). However, the mechanisms behind the isotopic fractionation during nitrogen fixation are not fully understood and it remains unclear why fluctuations in biomass  $\delta^{15}N$  occur under certain conditions but not others. Additionally, the effect of changing environmental conditions on the isotope effect of ‘alternative’ nitrogenase isozymes is poorly constrained.

A little studied control on the isotopic composition of nitrogen-fixer biomass is the release of newly fixed N. Marine and freshwater cyanobacteria are known to release nitrogen when growing diazotrophically (for example: Capone et al., 1994; Glibert and Bronk, 1994; Mulholland et al., 2004; Berthelot et al., 2015; Adam et al., 2016; Bonnet et al., 2016; Lu et al., 2018). The release of N can be substantial ( $>50\%$  of fixed N, Capone et al., 1994; Glibert and Bronk, 1994) and could affect biomass  $\delta^{15}N$ , were its isotopic composition distinct from that of biomass. However, to our knowledge, paired  $\delta^{15}N$  measurements of biomass and released nitrogen have not been conducted in pure cultures of any diazotroph. In light of previous reports that Fe limitation influences biomass  $\delta^{15}N$  (Zerkle et al., 2008), the possible role of nitrogen release is particularly intriguing as many bacteria are known to secrete high concentrations of N-rich Fe-binding molecules called siderophores under Fe limitation (Hider and Kong, 2010). If siderophores were distinct in  $\delta^{15}N$  relative to the biomass of the nitrogen fixer, their release could lead to the previ-

ously observed enrichment in biomass  $^{15}N$  under Fe limitation. Moreover, if nitrogen released by other diazotrophs is also isotopically distinct from biomass, such a mechanism could help to explain variations in field and laboratory measurements of biomass  $\delta^{15}N$  (Hoering and Ford, 1960; Wada and Hattori, 1976; Minagawa and Wada, 1986; Macko et al., 1987; Carpenter et al., 1997).

In this study, we (i) measure the effect of Fe limitation on biomass  $\delta^{15}N$  in the model nitrogen fixer *Azotobacter vinelandii*, (ii) determine the quantity as well as isotopic and chemical composition of released N, and (iii) use these data to assess changes in the isotopic composition of newly fixed nitrogen (the isotope effect).

*A. vinelandii* is a model nitrogen fixer, which encodes canonical (Mo) and alternative (Fe-only and V) nitrogenases (Bishop et al., 1986; Chisnell et al., 1988), allowing for comparisons between different isozymes. We grew wild type cultures supplied with Mo as well as mutants that encode only the Mo- or V-nitrogenase in order to explore nitrogen release when different nitrogenases were used. Previous studies have suggested that *Azotobacter spp.* release amino acids, vitamins, and  $NH_4^+$  during nitrogen fixation (Narula et al., 1981; Narula and Gupta, 1986; Gonzalez-Lopez et al., 1995; Revillas et al., 2000). *A. vinelandii* is also well studied for its production of siderophores (Corbin and Bulen, 1969; Page et al., 1991; Cornish and Page, 1995, 1998; Kraepiel et al., 2009), and we recently reported that under Fe limitation *A. vinelandii* can invest  $>30\%$  of fixed nitrogen in siderophore production (McRose et al., 2017). We measured the  $\delta^{15}N$  of biomass and released nitrogen in *Azotobacter vinelandii* cultures grown under Fe-limiting and Fe-replete conditions. Our results show that the  $\delta^{15}N$  of nitrogen released by *A. vinelandii* can be up to 3‰ lower than biomass. Under Fe-limiting conditions, siderophores are the majority of this released N and they are secreted in quantities large enough to elevate biomass  $\delta^{15}N$ . The  $^{15}N$  depletion in siderophores is consistent with the isotopic tendencies of the amino acids used in the biosynthesis of vibrioferrin and protochelin (the most abundant siderophores in our study), suggesting that other amino-acid derived siderophores are also likely to be depleted in  $^{15}N$  relative to the biomass of the organism that synthesized them.

## 2. METHODS

### 2.1. Bacterial strains and culture conditions

The wild type *Azotobacter vinelandii* strain OP as well as mutants that encode only the Mo-nitrogenase (CA1.70) or the V-nitrogenase (CA11.70) were grown in a nitrogen-free chemically defined medium (Bellenger et al., 2011) at 30 °C with shaking (100 RPM). For preliminary experiments, the growth medium was amended with 0.1  $\mu M$   $FeCl_3$  and 100 nM Mo or V. Further experiments were conducted in growth medium amended with 0.5  $\mu M$  or 5  $\mu M$   $FeCl_3$ , 0.16  $\mu M$  Mo or V and 100  $\mu M$  ethylenediaminetetraacetic acid (EDTA). Optical density was monitored throughout the experiment using the absorbance at 620 nm. All experiments were conducted using biological duplicates. For pre-

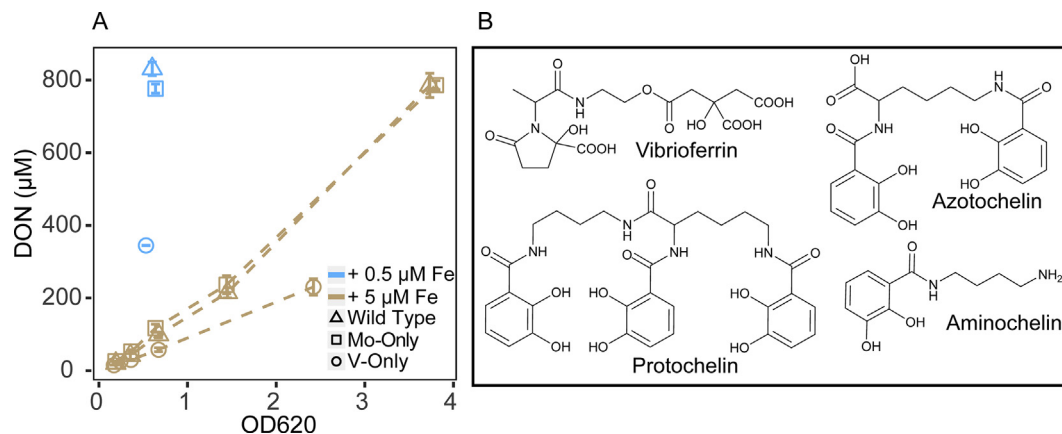


Fig. 1. Nitrogen release by nitrogen-fixing *A. vinelandii*. (A) Total nitrogen measured in cell-free supernatants of Mo-grown wild type (triangles), Mo-only mutant (squares), and V-only mutant (circles) cultures. Colors denote the initial iron concentration of the growth medium:  $0.5 \mu\text{M Fe}_T$  (blue) or  $5 \mu\text{M Fe}_T$  (brown). Nitrogen accumulations are shown as a function of optical density (OD measured at 620 nm) and are adjusted for nitrogen contributed by background EDTA present in the medium (see methods). The duration of experiments is  $\sim 36$  h (McRose et al., 2017). (B) Nitrogen containing siderophores produced by *A. vinelandii*. Additional siderophores DHBA and azotobactin are also synthesized by *A. vinelandii*. These are not shown because DHBA does not contain N, and azotobactin was not detected in our experiments.

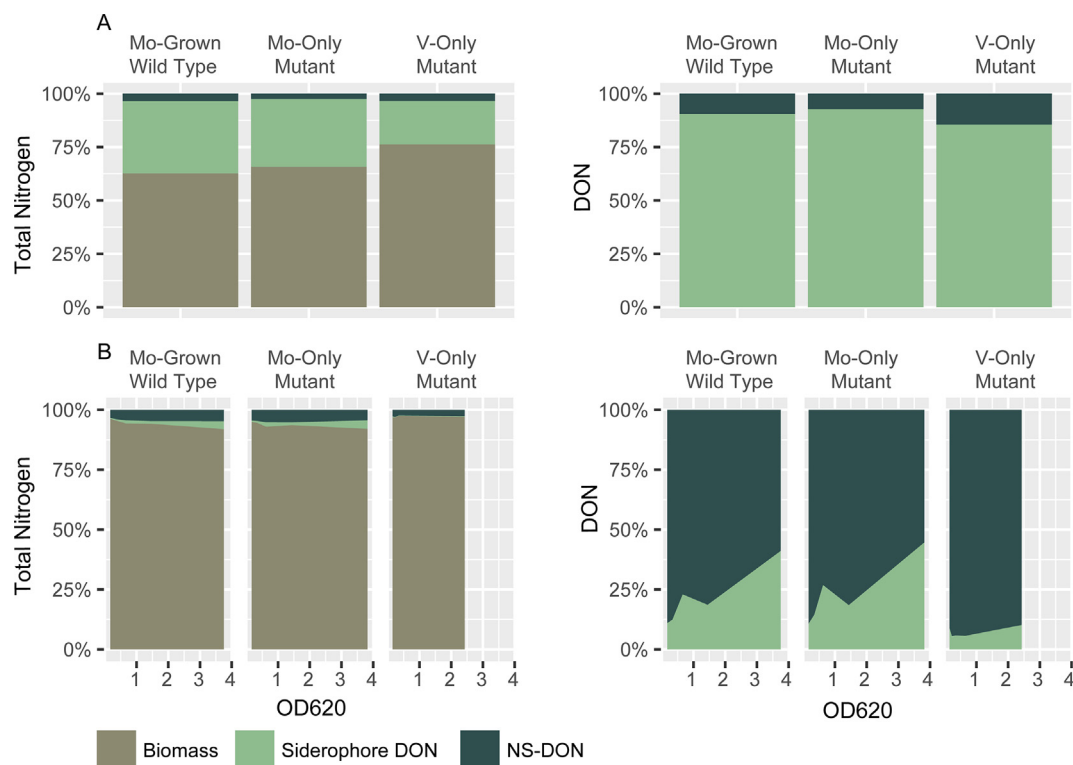


Fig. 2. Nitrogen budget for *A. vinelandii*. The proportion of nitrogen found as biomass (brown), siderophores (green) and NS-DON (dark green) is shown for: (A)  $0.5 \mu\text{M Fe}_T$ , (B)  $5 \mu\text{M Fe}_T$  treatments. The  $5 \mu\text{M Fe}_T$  treatment shows several points during growth, whereas the  $0.5 \mu\text{M Fe}_T$  treatment only shows one time point taken during stationary phase (OD = 0.5–0.6). Left hand panels show the composition of the total (biomass, siderophore DON, NS-DON) nitrogen pool, right hand panels show the composition of the dissolved nitrogen pool only. DON, dissolved organic nitrogen. NS-DON, non-siderophore dissolved organic nitrogen. Total fixed nitrogen (biomass and DON) concentrations were 1.4–2.3 mM ( $0.5 \mu\text{M Fe}_T$ ) and 7.7–9.9 mM ( $5 \mu\text{M Fe}_T$ ).

liminary experiments (Fig. S1), cells were collected during late exponential and early stationary phase for isotopic

analyses. In follow up experiments, cells were collected at the indicated optical density (Figs. 1–3).

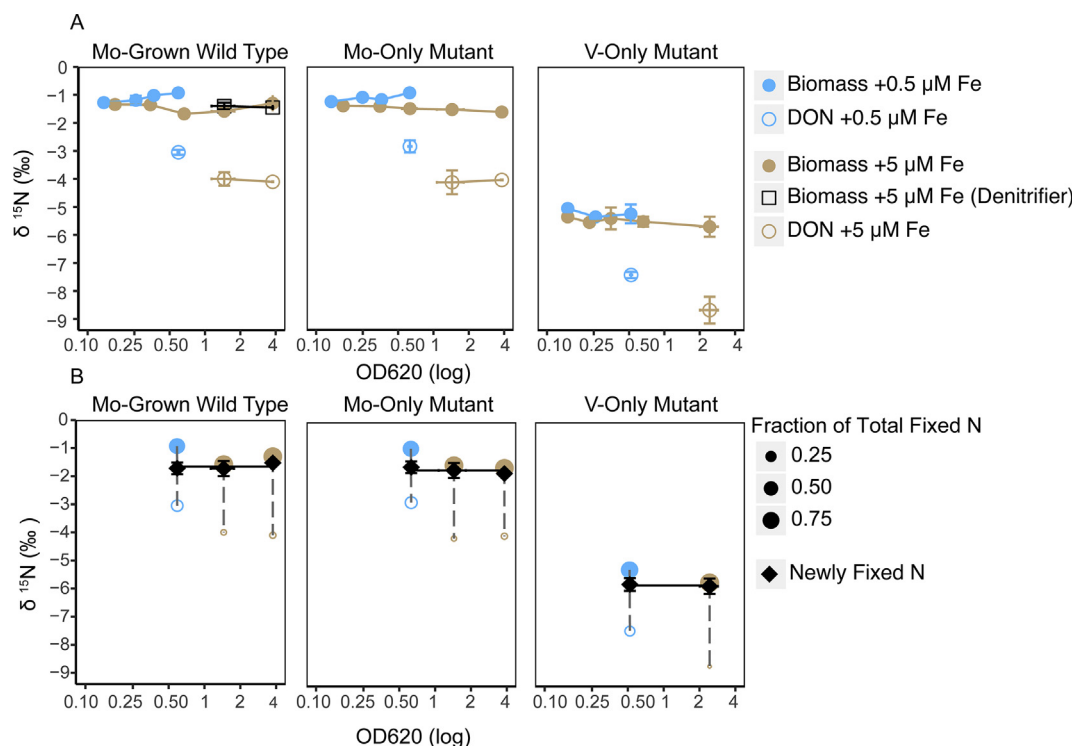


Fig. 3. Comparison of *A. vinelandii* particulate and dissolved nitrogen  $\delta^{15}\text{N}$ . (A) Dissolved organic nitrogen values (DON) and biomass  $\delta^{15}\text{N}$  for *A. vinelandii* cultures grown at 0.5  $\mu\text{M}$  (blue) and 5  $\mu\text{M}$  (brown)  $\text{Fe}_T$ . Biomass  $\delta^{15}\text{N}$  is shown with closed symbols, DON is shown with open symbols. Squares denote biomass samples measured using the denitrifier method (see methods). Samples were taken throughout growth and are shown as a function of optical density (OD). Due to Fe limitation, cells grown with 0.5  $\mu\text{M}$  Fe enter stationary phase at an OD of  $\sim 0.5$  whereas cells grown with 5  $\mu\text{M}$  Fe reach stationary phase at a much higher OD of  $\sim 2$ . Growth rates for Mo-grown cells were  $0.24 \pm 0.01 \text{ h}^{-1}$  at high Fe and  $0.11 \pm 0.01 \text{ h}^{-1}$  at low Fe, for the V-only mutant growth rates were  $0.16 \pm 0.01 \text{ h}^{-1}$  at high Fe and  $0.14 \pm 0.00 \text{ h}^{-1}$  at low Fe (McRose et al., 2017). When aligned vertically, biomass and DON values were determined from the same experiment. (B) Calculated  $\delta^{15}\text{N}$  of newly fixed nitrogen ( $\delta^{15}\text{N}_{\text{Nfix}}$ ), black triangles. Calculations were only performed for samples with matched DON and biomass isotope samples (Fig. 3A). Biomass and DON values from panel A are shown again and scaled according to their contribution to total fixed nitrogen. Error bars for  $\delta^{15}\text{N}_{\text{Nfix}}$  represent the propagated error (see methods). Error bars for DON and biomass  $\delta^{15}\text{N}$  are omitted in panel B for visual clarity. Standard deviations for biological duplicates are shown in all other cases ( $\pm$  SD). Data from this figure are presented in Table S3.

## 2.2. Measurement of biomass and released $\delta^{15}\text{N}$

Biomass samples for  $\delta^{15}\text{N}$  measurements were collected by filtration onto precombusted 25 mm glass microfiber filters (GF/F, Whatman, Maidstone, UK). Following filtration, samples were either lyophilized or dried at  $60^\circ\text{C}$  and both nitrogen content and  $\delta^{15}\text{N}$  were determined using an elemental analyzer (vario ISOTOPE cube, Elementar) coupled to an isotope ratio mass spectrometer (Isoprime 100, Isoprime, UK). Filters were rinsed with 20 mL of sterile salt solution (nitrogen-free medium without carbon, nitrogen, trace metals, and EDTA) to remove extracellular N. Rinsing was not performed for preliminary experiments (Fig. S1). In addition, wild type samples from the 5  $\mu\text{M}$  Fe treatments at two time points were also processed using the ‘denitrifier method’ (see below).

For released nitrogen analyses,  $\sim 10 \text{ mL}$  of *A. vinelandii* culture was centrifuged (3200g for 10 min at room temperature) and the resulting supernatant was filtered (0.22  $\mu\text{m}$ ) and frozen at  $-20^\circ\text{C}$ . Measurements of the OD620 of supernatants (after centrifugation but before filtration) showed

very low ODs suggesting that cells are efficiently pelleted and that the potential for cell lysis during syringe filtration is low (Fig. S2). All syringes (excluding stoppers) and centrifuge tubes used in experiments were acid washed (10% v/v hydrochloric acid) to remove any contaminating nitrogen. Preliminary experiments showed that this washing protocol was effective: milliQ blanks had background N concentrations  $< 3 \mu\text{M}$ . Sample nitrogen content and  $\delta^{15}\text{N}$  was determined by first oxidizing all sample nitrogen to nitrate (persulfate oxidation, as in Knapp et al., 2005) followed by the ‘denitrifier method’ (Sigman et al., 2001). For persulfate oxidation, 100  $\mu\text{L}$  of cell-free supernatant was combined with 2 mL of persulfate oxidizing reagent (POR), consisting of 2 g recrystallized potassium persulfate and 2 g ACS grade NaOH per 100 mL distilled deionized water. Samples were autoclaved for 1.5 hours at  $120^\circ\text{C}$  and sample pH was adjusted to  $\sim \text{pH}$  7 before bacterial conversion to  $\text{N}_2\text{O}$  and measurement on a Thermo MAT 253 isotope ratio mass spectrometer (Thermo Fisher Scientific, see Sigman et al., 2001; Weigand et al., 2016). In order to ensure complete oxidation of all nitrogen compounds in

our heterotrophic growth medium (which contains mM concentrations of organic carbon), known concentrations of L-glutamic acid (USGS40 and USGS41) were spiked into medium samples and their recovery was verified using the persulfate oxidation method (Fig. S3). Our growth medium utilizes the chelator EDTA, which is not metabolized by the cells but contributes ~200  $\mu\text{M}$  nitrogen. The concentration and isotopic composition of EDTA was determined in un-amended growth medium from each experiment (EDTA  $\delta^{15}\text{N}$  ranged from  $-0.94\text{‰}$  to  $+0.2\text{‰}$  due to changes in chemical batch) and was used to correct DON concentrations and isotopic values assuming linear mixing of EDTA and DON.

### 2.3. Quantification of siderophores, amino acids, $\text{NH}_4^+$ , and $\text{NO}_3^-$

Siderophores were quantified previously (McRose et al., 2017) using a single quadrupole LC-MS system (Agilent 6120, Agilent, Santa Clara, CA, USA), fitted with a UV-vis diode array detector. Supernatant samples were acidified and directly injected onto a C18 column (Agilent Eclipse Plus C18, 3.5  $\mu\text{m}$ , 4.6  $\times$  100 mm) without extraction. Separation was achieved using a gradient of A and B solutions (solution A: water + 0.1% formic acid + 0.1% acetic acid; solution B: acetonitrile + 0.1% formic acid + 0.1% acetic acid) over 30 min, at a flow rate of 0.8 mL/min. Vibrioferrin peak areas were quantified using calibration to an isolated standard. For catechol siderophores, UV chromatograms were extracted at 315 nm and concentrations were determined using known extinction coefficients (see Baars et al., 2015 and McRose et al., 2017). Quantification of free amino acids was performed at the Texas A&M protein chemistry lab.  $\text{NH}_4^+$  was measured using the orthophthaldialdehyde (OPA) method as described by (Holmes et al., 1999).  $\text{NO}_3^-$  concentrations were determined by reduction to NO and chemiluminescent detection (Braman and Hendrix, 1989).

### 2.4. Calculation of $\delta^{15}\text{N}_{\text{Nfix}}$ , kinetic isotope effect, and biomass sensitivity to N release

We calculated  $\delta^{15}\text{N}_{\text{Nfix}}$  using a linear mixing model of biomass and DON:

$$\delta^{15}\text{N}_{\text{Nfix}} = \delta^{15}\text{N}_{\text{DON}} \times f_{\text{DON}} + \delta^{15}\text{N}_{\text{bio}} \times f_{\text{bio}} \quad (1)$$

where  $\delta^{15}\text{N}_{\text{DON}}$  and  $\delta^{15}\text{N}_{\text{bio}}$  are the measured isotopic values of DON and biomass (Fig. 3A) and  $f_{\text{DON}}$  and  $f_{\text{bio}}$  are their fractional contributions to the total nitrogen pool (Fig. 2, Table S3). Error propagation for  $\delta^{15}\text{N}_{\text{Nfix}}$  was performed using a Monte Carlo method (implemented with the ‘propagate’ package in R, RCoreTeam) assuming the standard deviation for biomass  $\delta^{15}\text{N}_{\text{Nfix}}$  and DON  $\delta^{15}\text{N}$  are 0.4‰ (this was the largest observed for duplicate measurements of the same sample, the smallest observed sd was 0.04‰). Standard deviations for DON concentrations were assumed to be 20  $\mu\text{M}$  (the largest measured), standard deviations for biomass N concentrations were assumed to be 5% (the average observed in standards across multiple runs). The isotope effect,  $\epsilon_{\text{Nfix}}$ , was calculated by substitut-

ing  $\delta^{15}\text{N}_{\text{Nfix}}$  for  $\delta^{15}\text{N}_{\text{bio}}$  in the traditional definition ( $\epsilon_{\text{Nfix}} = \delta^{15}\text{N}_{\text{aq}} - \delta^{15}\text{N}_{\text{Nfix}}$ ) assuming average  $\delta^{15}\text{N}_{\text{Nfix}}$  values of  $-1.7\text{‰}$  and  $-5.8\text{‰}$  for the Mo- and V-isozymes (Table S3) and a  $\delta^{15}\text{N}_{\text{aq}}$  value of  $+0.7\text{‰}$ . Notably, a more complete calculation of these values using the isotope ratio ( $\alpha$ ) yields the same fractionation factors. Average siderophore DON and non-siderophore DON (NS-DON) isotope effects ( $\epsilon_{\text{Sid/bio}}$ ,  $\epsilon_{\text{NSDON/bio}}$ ) were determined by taking the regression of  $\epsilon_{\text{DON/bio}} = (\delta^{15}\text{N}_{\text{DON}} - \delta^{15}\text{N}_{\text{bio}})$  on the fraction of siderophores DON ( $f_{\text{sid}}$ ) and solving for  $f_{\text{sid}} = 1$  and  $f_{\text{sid}} = 0$  (end members). To determine the response of biomass  $\delta^{15}\text{N}$  to changes in nitrogen excretion and chemical composition we assumed that NS-DON was constitutively released as 4% of total nitrogen (as seen in our data, Fig. 2). Biomass, DON, NS-DON and siderophore DON  $\delta^{15}\text{N}$  were calculated as follows:

$$\delta^{15}\text{N}_{\text{bio}} = \delta^{15}\text{N}_{\text{Nfix}} - f_{\text{DON}} \times [f_{\text{Sid}} \times \epsilon_{\text{Sid/bio}} + (1 - f_{\text{Sid}}) \times \epsilon_{\text{NSDON/bio}}] \quad (2)$$

$$\delta^{15}\text{N}_{\text{Sid}} = \delta^{15}\text{N}_{\text{bio}} + \epsilon_{\text{Sid/bio}} \quad (3)$$

$$\delta^{15}\text{N}_{\text{NSDON}} = \delta^{15}\text{N}_{\text{bio}} + \epsilon_{\text{NSDON/bio}} \quad (4)$$

$$\delta^{15}\text{N}_{\text{DON}} = \delta^{15}\text{N}_{\text{bio}} + (f_{\text{Sid}} \times \epsilon_{\text{Sid/bio}}) + [(1 - f_{\text{Sid}}) \times \epsilon_{\text{NSDON/bio}}] \quad (5)$$

where  $\epsilon_{\text{Sid/bio}} = (\delta^{15}\text{N}_{\text{Sid}} - \delta^{15}\text{N}_{\text{bio}}) = -1.99$ ,  $\epsilon_{\text{NSDON/bio}} = (\delta^{15}\text{N}_{\text{NSDON}} - \delta^{15}\text{N}_{\text{bio}}) = -2.87$ , and  $f_{\text{Sid}} = \frac{f_{\text{DON}} - 0.04}{f_{\text{DON}}}$ .

## 3. RESULTS

### 3.1. Effect of Fe limitation on *A. vinelandii* biomass $\delta^{15}\text{N}$

In preliminary experiments (Fig. S1), we measured biomass  $\delta^{15}\text{N}$  from nitrogen-fixing *A. vinelandii* wild type (supplied with Mo) and V-only mutant cultures (supplied with V) grown under extreme Fe limitation ( $\text{Fe}_T = 0.1 \mu\text{M}$ ). As expected, cells using the V-nitrogenase had much lower biomass  $\delta^{15}\text{N}$  than those using the Mo-nitrogenase, reflecting the increased fractionation imparted by the alternative nitrogenase enzyme, as has been previously reported (Rowell et al., 1998; Zhang et al., 2014). Importantly, biomass  $\delta^{15}\text{N}$  of both the V-only and Mo-grown wild type cultures increased with successive transfers under Fe limitation, reaching a maximum value of  $+1.2\text{‰}$  for Mo-based nitrogen fixer biomass and  $-2.5\text{‰}$  for V-based nitrogen fixer biomass. These values are much higher than previously reported for *A. vinelandii* (ca.  $-1\text{‰}$  and  $-5.5\text{‰}$  for Mo and V nitrogenases, respectively, Rowell et al., 1998; Zhang et al., 2014).

### 3.2. Quantity and chemical composition of released nitrogen

Following our preliminary experiments, we quantified the release of fixed nitrogen by *A. vinelandii* Mo-grown wild type and Mo-only mutant cultures (hereafter Mo-grown cells) as well as V-only mutant cultures during growth in EDTA-buffered medium with varying concentrations of Fe ( $\text{Fe}_T = 0.5 \mu\text{M}$  or  $5 \mu\text{M}$ ). In our experiments, practically all of the extracellular nitrogen is organic (see below), as

such we refer to released nitrogen as Dissolved Organic Nitrogen (DON). Mo-grown cells released DON throughout the experiment and achieved similar final DON concentrations ( $\sim 800 \mu\text{M}$  after subtraction of nitrogen contributed by the chelator EDTA, see methods) across Fe-treatments. However, the DON release per cell (inferred from optical density, a proxy for cell count) was much greater in Fe-limited treatments (Fig. 1A). Nitrogen release in the V-only mutant was consistently lower than that of Mo-grown cells, but still varied with Fe.

Using total DON concentrations and known siderophore N concentrations (quantified by LC-MS and converted to N using siderophore structures, Fig. 1B, Table S1, McRose et al., 2017) we determined that siderophores represented a large fraction of the DON pool – with substantial differences between low and high Fe:  $<20\%$  at high Fe,  $>90\%$  at low Fe (compare Fig. 2A and B). Although previous studies have reported the excretion of  $\text{NH}_4^+$  and amino acids by *A. vinelandii*, (Narula et al., 1981; Narula and Gupta, 1986; Revillas et al., 2000) we found that these molecules only accounted for small fractions of the DON pool.  $\text{NH}_4^+$  was measured at the end of growth and found to be  $1\text{--}3 \mu\text{M}$  ( $\leq 1\%$  of the pool). Measurements of amino acids suggested that they also accounted for a small portion of the DON pool ( $\sim 6\%$  in representative samples), with alanine being the most abundant (Table S2). We also compared the concentrations of biomass N and DON in our experiments. As expected, the DON pool represented a much smaller fraction of total fixed nitrogen (biomass + DON) under Fe-replete as opposed to Fe-limited conditions (Fig. 2). At high Fe, the DON pool was small relative to biomass and was dominated by unidentified compounds (hereafter non-siderophore DON, ‘NS-DON’). In contrast, at low Fe, the DON pool was significantly larger and was dominated by siderophore DON (Fig. 2). Interestingly, the contribution of NS-DON to the total fixed nitrogen pool (DON and biomass) remained constant across treatments (Fig. 2).

### 3.3. Isotopic composition of DON and effect on biomass

Our data show that the  $\delta^{15}\text{N}$  of *A. vinelandii* biomass increases under Fe limitation (Fig. S1) and that DON release at low Fe can be substantial (Figs. 1 and 2). These results suggest that DON release could drive the observed changes in biomass  $\delta^{15}\text{N}$  at low Fe. To determine whether this is the case, we measured biomass  $\delta^{15}\text{N}$  and DON  $\delta^{15}\text{N}$  in samples from the same culture. Biomass  $\delta^{15}\text{N}$  was measured throughout growth and is shown as a function of OD (Fig. 3A). In agreement with our preliminary experiments (Fig. S1), Fe-limited Mo-grown cells had elevated biomass  $\delta^{15}\text{N}$  relative to Fe-replete Mo-grown cells. These values showed a slight but consistent increase throughout growth (likely due to increased Fe limitation as Fe became depleted in the medium, see below). DON  $\delta^{15}\text{N}$  was only measured late in growth when its concentrations greatly exceeded those of the chelator EDTA (which is added to control trace metal speciation but contributes  $\sim 200 \mu\text{M}$  background N, see methods). Nonetheless, in several cases,

we attained paired-DON  $\delta^{15}\text{N}$  measurements (aligned vertically in Fig. 3A). These measurements revealed that DON was indeed depleted in  $^{15}\text{N}$ : typically being  $\sim 2\text{--}3\%$  lower in  $\delta^{15}\text{N}$  than biomass in both Mo-grown cells and the V-only mutant (Fig. 3A). A set of biomass samples were also processed with the denitrifier method (used for DON measurements) and were found to be nearly identical to those determined using an EA-IRMS (used for biomass measurements), indicating that differences between biomass and DON  $\delta^{15}\text{N}$  cannot be attributed to methodological artifacts. The release of large quantities of  $^{15}\text{N}$ -depleted DON should elevate biomass  $\delta^{15}\text{N}$ .

In order to ensure that these changes in biomass  $\delta^{15}\text{N}$  are due to nitrogen release, we used the concentration data to calculate the fractions of newly fixed N being routed to released N ( $f_{\text{DON}}$ ) and biomass N ( $f_{\text{bio}}$ ), respectively (Fig. 2, Table S3). These were combined with their isotopic values ( $\delta^{15}\text{N}_{\text{DON}}$  and  $\delta^{15}\text{N}_{\text{bio}}$ , Fig. 3A) to calculate the  $\delta^{15}\text{N}$  of newly fixed N ( $\delta^{15}\text{N}_{\text{Nfix}}$ ):

$$\delta^{15}\text{N}_{\text{Nfix}} = \delta^{15}\text{N}_{\text{DON}} \times f_{\text{DON}} + \delta^{15}\text{N}_{\text{bio}} \times f_{\text{bio}} \quad (1)$$

This calculation showed that the  $\delta^{15}\text{N}$  of newly fixed N had a value of ca.  $-1.7\%$  for Mo-grown cells and ca.  $-5.8\%$  for the V-only mutant and that neither changed substantially across treatments (Fig. 3B, Table S3). Our calculated values for newly fixed N correspond to organism-level isotope effects ( $\epsilon_{\text{Nfix}}$ ) of  $\sim +2.4\%$ , and  $\sim +6.5\%$  for the Mo- and V-nitrogenase, respectively, with neither isotope effect showing a clear dependence on Fe status.

We also observed an elevation of DON  $\delta^{15}\text{N}$  in Mo-grown cells and the V-only mutant at  $0.5 \mu\text{M}$  Fe compared with  $5 \mu\text{M}$  Fe (Fig. 3A,B, blue leftmost DON point in each plot), which could correspond to a shift in the chemical composition of DON related to siderophore production (Fig. 2). To test this, we compared the difference of biomass  $\delta^{15}\text{N}$  and DON  $\delta^{15}\text{N}$  (essentially the ‘isotope effect’ of DON synthesis and release:  $\epsilon_{\text{DON/bio}} = \delta^{15}\text{N}_{\text{DON}} - \delta^{15}\text{N}_{\text{bio}}$ ) to the fraction of siderophore N found in the DON pool (Fig. 4A). Under conditions where cells release DON with a constant fractionation from biomass,  $\epsilon_{\text{DON/bio}}$  should remain unchanged. However,  $\epsilon_{\text{DON/bio}}$  was correlated ( $R^2 = 0.72$ ,  $p < 0.01$ ) with the siderophore contribution to DON (Fig. 4A, end member values are  $-1.99\%$  for pure siderophore DON and  $-2.87\%$  for pure NS-DON), implying that fluctuations in DON  $\delta^{15}\text{N}$  can be partly attributed to changes in siderophore concentrations.

## 4. DISCUSSION

Our results demonstrate that the organism-level, expressed kinetic isotope effect of nitrogen fixation does not change across Fe treatments. The variations in biomass  $\delta^{15}\text{N}$  in our experiments can be explained by changes in the partitioning of nitrogen between the biomass and DON pools (Figs. 3B, 4B, 5). Most strikingly, we observe an increase in biomass  $\delta^{15}\text{N}$  under Fe limitation, which results from the release of large amounts of  $^{15}\text{N}$ -depleted siderophore N. Shifts in both biomass  $\delta^{15}\text{N}$  and DON  $\delta^{15}\text{N}$  can

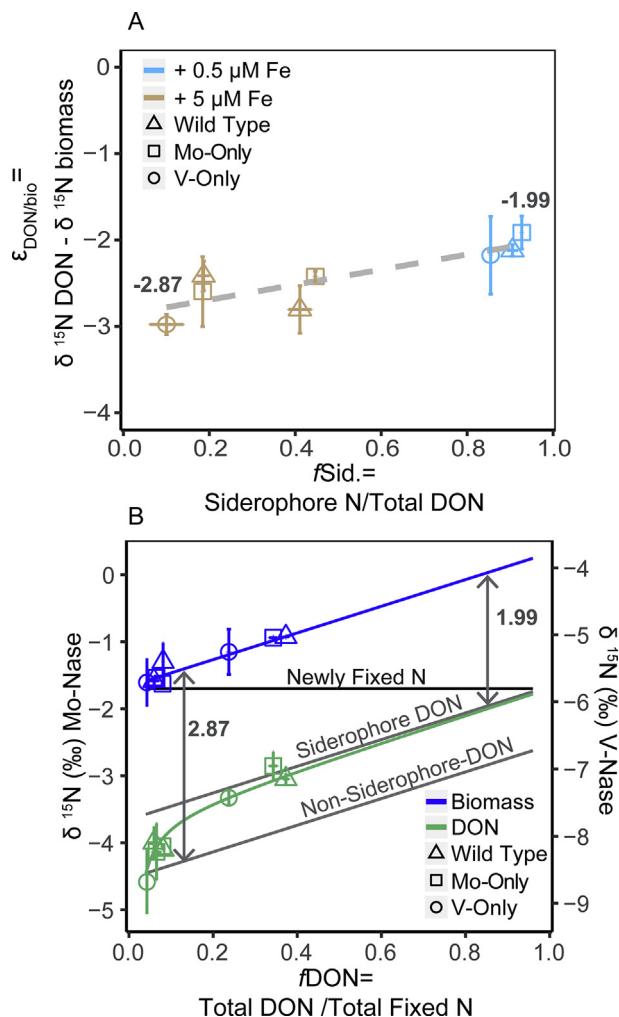


Fig. 4. Effect of DON chemical composition and quantity on biomass and DON  $\delta^{15}\text{N}$ . (A) Figure shows the difference between DON  $\delta^{15}\text{N}$  and biomass  $\delta^{15}\text{N}$  ( $\epsilon_{\text{DON/bio}}$ ) as a function of the percent of siderophore nitrogen in the DON pool. End member values are  $-2.87\text{‰}$  and  $-1.99\text{‰}$  for pure NS-DON and siderophores, respectively. Colors denote Fe present in growth medium (same as Figs. 1 and 3), symbols denote the mutant or wild type culture used (same as Fig. 1). The  $R^2$  value for the line of best fit is 0.72. (B) Sensitivity of biomass  $\delta^{15}\text{N}$  to changes in DON chemical composition and quantity. Modeled lines assume constitutive NS-DON release of 4% of total fixed nitrogen. Under this scenario, as the fraction of released DON increases, DON becomes dominated by siderophores. The green line denotes the DON value which is a combination of NS-DON and siderophores. The blue line denotes biomass  $\delta^{15}\text{N}$  which is shifted up due to the constitutive release of NS-DON and increases linearly as a function of DON release (which is driven by siderophores). Symbols denote measured  $\delta^{15}\text{N}$  for mutant and wild type cultures (same as Figs. 1, 4A). Values for the Mo-nitrogenase are shown on the left-hand y-axis, those for the V-nitrogenase are shown on the right-hand y-axis. Error bars represent the standard deviation for biological duplicates. (For interpretation of the references to colour in this figure legend, the reader is referred to the web version of this article.)

therefore occur without alteration of the isotope effect of nitrogen fixation (Fig. 3A,B). It is possible that this mechanism is the sole cause for the observed shift towards higher

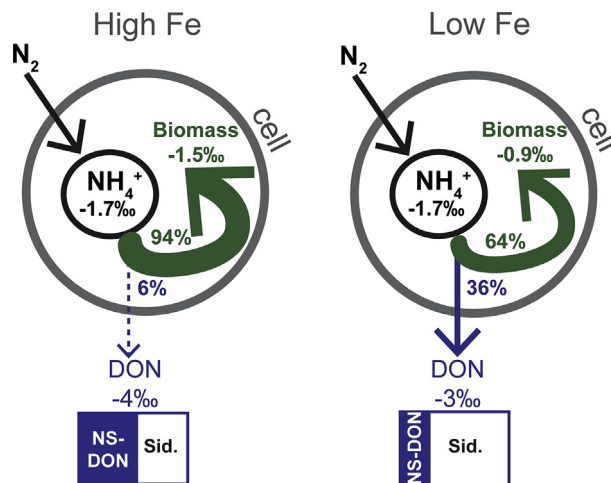


Fig. 5. Cartoon schematic of nitrogen release in *A. vinelandii*. At high Fe, nitrogen release is small and has very little effect on biomass  $\delta^{15}\text{N}$  and siderophores make up a small fraction of the DON pool. At low Fe, nitrogen release is large enough to affect biomass  $\delta^{15}\text{N}$ , and siderophores comprise the majority of the DON pool. NS-DON: non-siderophore dissolved organic nitrogen, Sid: siderophore nitrogen. Slight changes in DON  $\delta^{15}\text{N}$  are due to changes in the flux of DON and the chemical composition of the DON pool (Fig. 4).

biomass  $\delta^{15}\text{N}$  over the entire range of growth rates ( $0.02$ – $0.25 \text{ h}^{-1}$ , Fig. S1) observed in our experiments, suggesting that the organismal isotope effect of nitrogen fixation remains constant even at very slow growth rates; a result that stands in contrast to studies of sulfate reduction where metabolic rate (and by extension growth rate) has been found to influence the isotope effect (Sim et al., 2011; Leavitt et al., 2013). Experiments exploring extremely low growth rates in nitrogen fixers are needed to verify this finding. Nevertheless, the very large difference in the isotope effects of Mo- and V-nitrogenases is clearly maintained even in cases when Mo-grown cells and the V-only mutant have similar growth rates (Fig. S1), implying that these different fractionations are intrinsic to the different nitrogenase isozymes. The stability of the isotope effect for nitrogen fixation by a given nitrogenase is a positive outcome for the use of the N isotopes to reconstruct the fixed N budget on land (Houlton and Bai, 2009) and in the ocean (Brandes and Devol, 2002).

#### 4.1. Effect of Fe limitation on $\delta^{15}\text{N}$ of biomass, DON, and newly fixed N

One complex feature of our data is the elevation in DON  $\delta^{15}\text{N}$  at low Fe (Fig. 3A). This results from a combination of two factors that accompany Fe limitation (i) increases in the DON flux (due to siderophore production) and (ii) changes in the isotopic composition of DON (also due to siderophore production). As the flux of DON becomes large at low Fe, biomass  $\delta^{15}\text{N}$  increases away from newly fixed N, and DON  $\delta^{15}\text{N}$  undergoes a concomitant increase toward newly fixed N. Moreover, although siderophores and NS-DON are chemically complex pools, our data also

suggest that siderophores may have a slightly smaller fractionation relative to biomass ( $-1.99\text{‰}$  for siderophore DON vs.  $-2.87\text{‰}$  for NS-DON, Fig. 4A), and as a result have a slightly higher  $\delta^{15}\text{N}$  than the NS-DON pool. This presents a driver for nitrogen fixer-derived DON to increase in  $\delta^{15}\text{N}$  under low Fe. These findings represent a cautionary note against the interpretation of any local decline in DON  $\delta^{15}\text{N}$  as an indication of higher nitrogen fixation: DON  $\delta^{15}\text{N}$  may decline under Fe-rich conditions without any increase in nitrogen fixation rate, simply because of the shift away from siderophore production. Analogously, any change (increase) in biomass  $\delta^{15}\text{N}$  may not result from decreases in nitrogen fixation rate, but instead from alteration of the cellular N isotope budget in response to Fe availability.

We explored the effects of siderophore and NS-DON release on biomass  $\delta^{15}\text{N}$  using a simple model (see methods for details). Our measurements of DON chemical composition (Fig. 2) suggest that NS-DON is released as a relatively consistent fraction of total fixed nitrogen ( $\sim 4.3\%$  for Mo-based nitrogen fixers and  $\sim 2.8\%$  for V-based nitrogen fixation). Assuming that NS-DON is released constantly as 4% of total fixed N and using our calculated isotope effects for the synthesis of siderophore DON and NS-DON (Fig. 4A), we modeled DON and biomass  $\delta^{15}\text{N}$  as a function of the DON flux. In this model (and in our data) DON  $\delta^{15}\text{N}$  responds non-linearly to changes in the DON flux: NS-DON represents 100% of the DON pool when DON fluxes are low, but only a small fraction of the pool when DON fluxes are high. Biomass  $\delta^{15}\text{N}$  nonetheless has a linear response to changes in the DON flux because both NS-DON and siderophore DON are released proportionally with respect to biomass. Overall, DON  $\delta^{15}\text{N}$  must become enriched in  $^{15}\text{N}$  at low Fe simply due to the increase in DON flux (Fig. 4B). However, siderophores serve to further enrich DON in  $^{15}\text{N}$  and notably, lead to more modest elevations in biomass  $\delta^{15}\text{N}$  than expected if the DON pool were dominated by (more  $^{15}\text{N}$ -depleted) NS-DON.

This model fits our data well and suggests a maximum biomass  $\delta^{15}\text{N}$  of  $\sim +0.3\text{‰}$  when 100% of fixed nitrogen is routed to DON (a theoretical upper bound as it precludes biomass production entirely). This value is lower than the  $+1.2\text{‰}$  value for (Mo-nitrogenase) biomass  $\delta^{15}\text{N}$  seen in our preliminary studies, which were conducted under extreme Fe limitation. This very high biomass  $\delta^{15}\text{N}$  could reflect shifts in the kinetic isotope effect that occur only under extreme Fe limitation. Barring this possibility, another explanation could be the secretion of different siderophores that are slightly more depleted in  $^{15}\text{N}$ . Indeed, under extreme Fe limitation, *A. vinelandii* is known to make the large siderophore azotobactin (Bulen and LeComte, 1962; Page et al., 1991; Kraepiel et al., 2009; Yoneyama et al., 2011; Baars et al., 2015). Although azotobactin was not produced in our  $0.5\ \mu\text{M}$  Fe treatments, it has been observed in supernatants from cells cultured with  $0.1\ \mu\text{M}$   $\text{Fe}_T$  (Baars et al., 2015) and would most likely have been produced in our preliminary experiments. Were azotobactin depleted in  $^{15}\text{N}$  relative to vibrioferrin and protochelin (the main siderophores produced in our  $0.5\ \mu\text{M}$  and  $5\ \mu\text{M}$  Fe treatments), it could lead to the observed biomass  $\delta^{15}\text{N}$ .

Based on our findings, we propose  $\sim +1\text{‰}$  as an upper limit for biomass  $\delta^{15}\text{N}$  under Fe limitation.

#### 4.2. Mechanisms underlying $^{15}\text{N}$ depletion in siderophore and NS-DON

Siderophores account for a major fraction of DON in our Fe-limited experiments and due to their low  $\delta^{15}\text{N}$ , they have a large influence on biomass  $\delta^{15}\text{N}$ . This  $^{15}\text{N}$  depletion in siderophores can be readily understood in terms of the amino acid precursors used in siderophore biosynthesis. Newly fixed N is incorporated into amino acids via the glutamine synthetase-glutamine oxoglutarate aminotransferase (GS/GOGAT) cycle, following which it can be used to build various amino acids via transamination reactions. Transamination transfers the  $^{14}\text{N}$  isotope more quickly than the heavy  $^{15}\text{N}$  isotope, allowing for some amino acids to become depleted in  $^{15}\text{N}$  (Macko et al., 1986). This appears to be the case for the amino acids used to build vibrioferrin and protochelin (Fig. 1B), two of the most abundant siderophores in our experiments (Table S1). The two nitrogen atoms in vibrioferrin come from alanine and serine (Tanabe et al., 2003; Challis, 2005). Protochelin obtains two nitrogen atoms from lysine and two from butane 1,4-diamine (putrescine), a breakdown product of arginine (Yoneyama et al., 2011; Baars et al., 2015). Empirical investigations of *de novo* microbial amino acid synthesis have shown that alanine and arginine often have  $\delta^{15}\text{N}$  close to their nitrogen source but that lysine and serine are often depleted in  $^{15}\text{N}$  (Macko et al., 1987; McClelland and Montoya, 2002; Chikaraishi et al., 2009; McCarthy et al., 2013); the incorporation of these amino acids should therefore lead to a decrease in siderophore  $\delta^{15}\text{N}$ , as we observed. The use of amino acid precursors is common in siderophore biosynthesis (Hider and Kong, 2010) suggesting that many other amino acid-derived siderophores will be depleted in  $^{15}\text{N}$  relative to the biomass that produced them.

The composition of the NS-DON pool remains unknown. Potential contributors to this pool are any N-containing organic molecules not measured in our study: small peptides, larger proteins, vitamins, nucleic acids, secondary metabolites, non-proteinogenic amino acids, or polyamines. If NS-DON is peptidic or proteinaceous the reason for its release remains unclear. Preliminary searches for vitamins suggested they were not present in high concentrations. Nucleic acids can also be released by bacteria; especially during biofilm formation (Flemming and Wingender, 2010). And there is some evidence for increased *A. vinelandii* competence (and potentially DNA release) under diazotrophic conditions (Page and Sadoff, 1976). It is extremely unlikely that NS-DON results from heretofore unrecognized *A. vinelandii* siderophores (Baars et al., 2014; Baars et al., 2015). Other secondary metabolites such as antibiotics often contain nitrogen and could also contribute to NS-DON. However, the fact that NS-DON is released very consistently across treatments suggests that it may represent a waste or intermediate product associated with growing cells rather than a more specialized secondary metabolite. Non-proteinogenic amino acids such as ornithine or polyamines such as putrescine, spermidine, or

spermine produced during amino acid breakdown could also contribute to NS-DON. We did not detect significant amounts of putrescine in our culture supernatants, although the presence of other compounds was not measured. However, there is some evidence for the production (but not excretion) of polyamines in *Azotobacter* species grown under diazotrophic conditions (Goris et al., 1998) and for the accumulation of di- and polyamines in other microbial cultures (Herbst et al., 1958; Kashiwagi et al., 1992; Yodsang et al., 2014). If these are indeed the constituents of NS-DON, their low  $\delta^{15}\text{N}$  might have a similar explanation to that of siderophore DON: transamination or deamination during biosynthesis of the molecules (or their amino acid precursors) could lead to  $^{15}\text{N}$ -depletion.

It is also notable that our measurements of both siderophore and NS-DON are depleted in  $^{15}\text{N}$ , whereas environmental measurements of marine DON (which can be less complex to interpret than those from terrestrial systems) are often enriched in  $^{15}\text{N}$  relative to biomass (Knapp et al., 2005; Meador et al., 2007; Knapp et al., 2012). *A. vinelandii*, a soil bacterium, may not be representative of processes occurring in marine systems. However, assuming that our observations can be generalized, they suggest that DON  $\delta^{15}\text{N}$  in these systems is set by fractionation during assimilation or further degradation of DON, but not by its excretion from cells.

#### 4.3. Differences in N release between *A. vinelandii* cultures using Mo- and V-nitrogenases

Our data show that *A. vinelandii* releases substantial amounts of fixed nitrogen. Consistent with previous publications,  $\text{NH}_4^+$  and amino acids were part of this nitrogen pool (Narula et al., 1981; Narula and Gupta, 1986; Gonzalez-Lopez et al., 1995; Revillas et al., 2000) but our data show that  $\text{NH}_4^+$  and amino acids were present at much lower concentrations than siderophores and NS-DON. We also observed differences in the amount of DON released by cultures using the V- as opposed to Mo-nitrogenase (Figs. 1 and 2). The V-nitrogenase is known to be less efficient than the Mo-nitrogenase and cultures using this nitrogenase have slower growth rates than those using the Mo-nitrogenase (Eady and Robson, 1984; Bellenger et al., 2011). We previously noted that *A. vinelandii* produces fewer siderophores when using the V- as opposed to Mo-nitrogenase and we suggested that on account of their slow growth rates V-only mutants may be able to take up Fe more slowly, allowing for a decrease in siderophore production (McRose et al., 2017). Another possible explanation is that *A. vinelandii* curtails N release when using the V-nitrogenase in order to compensate for the lower efficiency of this nitrogenase isozyme. Our current finding that the entire DON pool (not just siderophores) is smaller in the V-nitrogenase mutant (Figs. 1 and 2) lends support to this second hypothesis. The difference in DON release between cultures employing different isozymes also implies that *A. vinelandii* cells using the Mo-nitrogenase fix more nitrogen than is needed for biomass production and release the excess N. This process may also occur during Mo-based nitrogen fixation in other diazotrophs and could help

explain previous observations of N release by diazotrophs (e.g. Capone et al., 1994; Glibert and Bronk, 1994; Mulholland et al., 2004; Berthelot et al., 2015; Adam et al., 2016; Bonnet et al., 2016; Lu et al., 2018). The potential benefits of this process for the nitrogen fixer, and possibly co-occurring bacteria, remain unknown.

#### 4.4. Additional implications for interpretation of biomass $\delta^{15}\text{N}$ and nitrogen fixation rates

Natural abundance isotope studies provide valuable insights into nitrogen cycling. We show that DON release can decouple the isotope effect of N fixation from cellular isotopic composition, potentially increasing the  $\delta^{15}\text{N}$  of nitrogen-fixer biomass up to +1.2‰ (Fig. S1). Measurements of diazotrophic biomass  $\delta^{15}\text{N}$  from both field and lab experiments often exhibit substantial variations (Hoering and Ford, 1960; Wada and Hattori, 1976; Minagawa and Wada, 1986; Macko et al., 1987; Carpenter et al., 1997). Our findings point to nitrogen release, a process not previously quantified in isotope studies, as a possible driver of this variation. In addition to the consequences for natural abundance isotope studies, the release of large amounts of DON can also affect the  $^{15}\text{N}_2$  tracer-based measurement of nitrogen fixation rates, leading to underestimates when rates are determined via isotopic label ( $^{15}\text{N}_2$ ) incorporation, as has been previously shown in marine systems (Mulholland et al., 2004).

Siderophore production is extremely common in both marine and terrestrial heterotrophic bacteria (Hider and Kong, 2010), and also occurs in freshwater phototrophs such as *Anabaena variabilis* (Trick and Kerry, 1992) and *Rhodospseudomonas palustris* (Larimer et al., 2004; Baars et al., 2018). Given what is known about siderophore biosynthesis, it is possible that these organisms release low  $\delta^{15}\text{N}$  N via siderophores, as observed in *A. vinelandii*. In fact, as suggested by Zerkle et al. (2008), siderophore release may contribute to the previous observation that *A. variabilis* exhibits increased biomass  $\delta^{15}\text{N}$  under Fe limitation. While important marine diazotrophs such as *Trichodesmium* have not been found to synthesize siderophores (Hopkinson and Morel, 2009), these organisms have been shown to release fixed nitrogen (Capone et al., 1994; Glibert and Bronk, 1994; Mulholland et al., 2004; Berthelot et al., 2015; Bonnet et al., 2016; Lu et al., 2018), often in the form of amino acids. The isotopic composition of this released nitrogen has yet to be explored in pure culture systems. However, our study provides a proof of concept that DON can in fact alter biomass  $\delta^{15}\text{N}$  and suggests that this process may occur in other diazotrophs.

The fate of released N is a key question in assessing its potential effects on N isotopic distributions in the environment and their use to study modern and past nitrogen cycling. For example, if siderophores are assimilated by other organisms, as intact compounds or after degradation, they may have an effect on the  $\delta^{15}\text{N}$  of other organisms in the environment that is more immediate than through trophic transfers of biomass N. In the ocean, if released N is preferentially recycled in the surface while N fixer biomass is preferentially exported from the surface ocean, the

impact of N fixation on water column N isotope distributions will be different than without this discrepancy in fates. Such variations in biomass versus DON  $\delta^{15}\text{N}$  are potentially relevant for recent investigations of organic nitrogen isotopes in shales (for example Stüeken et al., 2015; Zerkle et al., 2017; Li et al., 2018). Perhaps most intriguingly, in the case of siderophore producers, if a well-preserved, N-bearing biomarker of N fixers is identified, the  $\delta^{15}\text{N}$  of this biomarker might reveal past variations in the iron limitation of nitrogen fixation.

## 5. CONCLUSION

We have shown that nitrogen release can decouple biomass  $\delta^{15}\text{N}$  measurements from the kinetic isotope effect of nitrogen fixation. To our knowledge, this is the first evidence from culture-based studies that released nitrogen is  $^{15}\text{N}$ -depleted and produced in adequate quantities to alter biomass  $\delta^{15}\text{N}$ . In *A. vinelandii*, N-release is primarily driven by siderophore secretion, a process that is well understood and provides a molecular rationale for the low  $\delta^{15}\text{N}$  of DON: *A. vinelandii* siderophores are synthesized from amino acids that are known to be  $^{15}\text{N}$  depleted. Comparisons of N-release during Mo- and V-based nitrogen fixation also raise the possibility that ‘over-fixation’ by the more efficient Mo-nitrogenase facilitates N release in *A. vinelandii* and other diazotrophs. Our work suggests that the release of low  $\delta^{15}\text{N}$  nitrogen affects the interpretation of biomass  $\delta^{15}\text{N}$  measurements made in both laboratory and environmental settings and offers mechanistic insights into this process.

## ACKNOWLEDGEMENTS

We thank M.A. Weigand for her help and guidance with the denitrifier method. We are also grateful to X.T. Wang, E.R. Kast, V. Luu, J.A. Lueders-Dumont, S.E. Fawcett and A.R. Babbitt for helpful discussions and assistance with methods. This work was supported by the Princeton Environmental Institute, the National Science Foundation (grant numbers EAR-1631814 and OCE 1657639) and NASA 80NSSC17K0667.

## APPENDIX A. SUPPLEMENTARY MATERIAL

Supplementary data to this article can be found online at <https://doi.org/10.1016/j.gca.2018.09.023>.

## REFERENCES

- Adam B., Klawonn I., Svedén J. B., Bergkvist J., Nahar N., Walve J., Littmann S., Whitehouse M. J., Lavik G., Kuypers M. M. M. and Ploug H. (2016)  $\text{N}_2$ -fixation, ammonium release and N-transfer to the microbial and classical food web within a plankton community. *ISME J.* **10**, 450–459.
- Baars O., Morel F. M. M. and Perlman D. H. (2014) ChelomEx: isotope-assisted discovery of metal chelates in complex media using high-resolution LC-MS. *Anal. Chem.* **86**, 11298–11305.
- Baars O., Zhang X., Morel F. M. M. and Seyedsayamdost M. R. (2015) The siderophore metabolome of *Azotobacter vinelandii*. *Appl. Environ. Microbiol.* **82**, 27–39.
- Baars O., Morel F. M. M. and Zhang X. (2018) The purple non-sulfur bacterium *Rhodospseudomonas palustris* produces novel petrobactin-related siderophores under aerobic and anaerobic conditions. *Environ. Microbiol.* **130**, 2124.
- Beaumont V. I., Jahnke L. L. and Des Marais D. J. (2000) Nitrogen isotopic fractionation in the synthesis of photosynthetic pigments in *Rhodobacter capsulatus* and *Anabaena cylindrica*. *Org. Geochem.* **31**, 1075–1085.
- Bellenger J. P., Wichard T., Xu Y. and Kraepiel A. M. L. (2011) Essential metals for nitrogen fixation in a free-living  $\text{N}_2$ -fixing bacterium: chelation, homeostasis and high use efficiency. *Environ. Microbiol.* **13**, 1395–1411.
- Berthelot H., Bonnet S., Camps M., Grosso O. and Moutin T. (2015) Assessment of the dinitrogen released as ammonium and dissolved organic nitrogen by unicellular and filamentous marine diazotrophic cyanobacteria grown in culture. *Front. Mar. Sci.* **2**, 2233.
- Bishop P. E., Premakumar R., Dean D. R., Jacobson M. R., Chisnell J. R., Rizzo T. M. and Kopczynski J. (1986) Nitrogen fixation by *Azotobacter vinelandii* strains having deletions in structural genes for nitrogenase. *Science* **232**, 92–94.
- Bonnet S., Berthelot H., Turk-Kubo K., Fawcett S., Rahav E., L’Helgouen S. and Berman-Frank I. (2016) Dynamics of  $\text{N}_2$  fixation and fate of diazotroph-derived nitrogen in a low-nutrient, low-chlorophyll ecosystem: results from the VAHINE mesocosm experiment (New Caledonia). *Biogeosciences* **13**, 2653–2673.
- Braman R. S. and Hendrix S. A. (1989) Nanogram nitrite and nitrate determination in environmental and biological materials by vanadium (III) reduction with chemiluminescence detection. *Anal. Chem.* **61**, 2715–2718.
- Brandes J. A. and Devol A. H. (2002) A global marine-fixed nitrogen isotopic budget: implications for Holocene nitrogen cycling. *Global Biogeochem. Cycles* **16**, 67–61–67–14.
- Bulen W. A. and LeComte J. R. (1962) Isolation and properties of a yellow-green fluorescent peptide from *Azotobacter* medium. *Biochem. Biophys. Res. Commun.* **9**, 523–528.
- Capone D. G., Ferrier M. D. and Carpenter E. J. (1994) Amino acid cycling in colonies of the planktonic marine cyanobacterium *Trichodesmium thiebautii*. *Appl. Environ. Microbiol.* **60**, 3989–3995.
- Carpenter E. J., Harvey H. R., Fry B. and Capone D. G. (1997) Biogeochemical tracers of the marine cyanobacterium *Trichodesmium*. *Deep Sea Res. Part I: Oceanogr. Res. Papers* **44**, 27–38.
- Challis G. L. (2005) A widely distributed bacterial pathway for siderophore biosynthesis independent of nonribosomal peptide synthetases. *ChemBioChem* **6**, 601–611.
- Chikaraishi Y., Ogawa N. O., Kashiyama Y., Takano Y., Suga H., Tomitani A., Miyashita H., Kitazato H. and Ohkouchi N. (2009) Determination of aquatic food-web structure based on compound-specific nitrogen isotopic composition of amino acids. *Limnol. Oceanogr. Methods* **7**, 740–750.
- Chisnell J. R., Premakumar R. and Bishop P. E. (1988) Purification of a second alternative nitrogenase from a *nifHDK* deletion strain of *Azotobacter vinelandii*. *J. Bacteriol.* **170**, 27–33.
- Corbin J. L. and Bulen W. A. (1969) Isolation and identification of 2,3-dihydroxybenzoic acid and 2-N,6-N-Di(2,3-dihydroxybenzoyl)-L-lysine formed by iron-deficient *Azotobacter vinelandii*. *Biochemistry* **8**, 757–762.
- Cornish A. S. and Page W. J. (1995) Production of the triacetate siderophore protochelin by *Azotobacter vinelandii*. *Biomaterials* **8**, 332–338.
- Cornish A. S. and Page W. J. (1998) The catecholate siderophores of *Azotobacter vinelandii*: their affinity for iron and role in oxygen stress management. *Microbiology* **144**, 1747–1754.

- Eady R. R. and Robson R. L. (1984) Characteristics of N<sub>2</sub> fixation in Mo-limited batch and continuous cultures of *Azotobacter vinelandii*. *Biochem. J.* **224**, 853–862.
- Flemming H.-C. and Wingender J. (2010) The biofilm matrix. *Nat. Rev. Microbiol.* **8**, 623–633.
- Glibert P. M. and Bronk D. A. (1994) Release of dissolved organic nitrogen by marine diazotrophic cyanobacteria, *Trichodesmium* spp. *Appl. Environ. Microbiol.* **60**, 3996–4000.
- Gonzalez-Lopez J., Martinez-Toledo M. V., Rodelas B., Pozo C. and Salmerón V. (1995) Production of amino acids by free-living heterotrophic nitrogen-fixing bacteria. *Amino Acids* **8**, 15–21.
- Goris J., Kersters K. and De Vos P. (1998) Polyamine distribution among authentic Pseudomonads and *Azotobacteraceae*. *Syst. Appl. Microbiol.* **21**, 285–290.
- Gruber N. and Galloway J. N. (2008) An Earth-system perspective of the global nitrogen cycle. *Nature* **451**, 293–296.
- Herbst E. J., Weaver R. H. and Keister D. L. (1958) The gram reaction and cell composition: diamines and polyamines. *Arch. Biochem. Biophys.* **75**, 171–177.
- Hider R. C. and Kong X. (2010) Chemistry and biology of siderophores. *Nat. Prod. Rep.* **27**, 637–657.
- Hoering T. C. and Ford H. T. (1960) The isotope effect in the fixation of nitrogen by *Azotobacter*. *J. Am. Chem. Soc.* **82**, 376–378.
- Holmes R. M., Aminot A., Kérouel R., Hooker B. A. and Peterson B. J. (1999) A simple and precise method for measuring ammonium in marine and freshwater ecosystems. *Can. J. Fish. Aquat. Sci.* **56**, 1801–1808.
- Hopkinson B. M. and Morel F. M. M. (2009) The role of siderophores in iron acquisition by photosynthetic marine microorganisms. *Biometals* **22**, 659–669.
- Houlton B. Z. and Bai E. (2009) Imprint of denitrifying bacteria on the global terrestrial biosphere. *PNAS* **106**, 21713–21716.
- Kashiwagi K., Miyamoto S., Suzuki F., Kobayashi H. and Igarashi K. (1992) Excretion of putrescine by the putrescine-ornithine antiporter encoded by the potE gene of *Escherichia coli*. *PNAS* **89**, 4529–4533.
- Klots C. E. and Benson B. B. (1963) Isotope effect in the solution of oxygen and nitrogen in distilled water. *J. Chem. Phys.* **38**, 890–892.
- Knapp A. N., Sigman D. M. and Lipschultz F. (2005) N isotopic composition of dissolved organic nitrogen and nitrate at the Bermuda Atlantic Time-series Study site. *Global Biogeochem. Cycles* **19**, 1.
- Knapp A. N., Sigman D. M., Kustka A. B., Sañudo-Wilhelmy S. A. and Capone D. G. (2012) The distinct nitrogen isotopic compositions of low and high molecular weight marine DON. *Mar. Chem.* **136–137**, 24–33.
- Kraepiel A. M. L., Bellenger J. P., Wichard T. and Morel F. M. M. (2009) Multiple roles of siderophores in free-living nitrogen-fixing bacteria. *Biometals* **22**, 573–581.
- Larimer F. W., Chain P., Hauser L., Lamerdin J., Malfatti S., Do L., Land M. L., Pelletier D. A., Beatty J. T., Lang A. S., Tabita F. R., Gibson J. L., Hanson T. E., Bobst C., Torres J. L. T. Y., Peres C., Harrison F. H., Gibson J. and Harwood C. S. (2004) Complete genome sequence of the metabolically versatile photosynthetic bacterium *Rhodospseudomonas palustris*. *Nat. Biotechnol.* **22**, 55–61.
- Leavitt W. D., Halevy I., Bradley A. S. and Johnston D. T. (2013) Influence of sulfate reduction rates on the Phanerozoic sulfur isotope record. *PNAS* **110**, 11244–11249.
- Li M., Chen J., Wang T., Zhong N. and Shi S. (2018) Nitrogen isotope and trace element composition characteristics of the Lower Cambrian Niutitang Formation shale in the upper - middle Yangtze region, South China. *Palaeogeogr. Palaeoclimatol. Palaeoecol.* **501**, 1–12.
- Lu Y., Wen Z., Shi D., Chen M., Zhang Y., Bonnet S., Li Y., Tian J. and Kao S.-J. (2018) Effect of light on N<sub>2</sub> fixation and net nitrogen release of *Trichodesmium* in a field study. *Biogeosciences* **15**, 1–12.
- Macko S. A., Estep M. L. F., Engel M. H. and Hare P. E. (1986) Kinetic fractionation of stable nitrogen isotopes during amino acid transamination. *Geochem. Cosmochim. Acta* **50**, 2143–2146.
- Macko S. A., Fogel M. L., Hare P. E. and Hoering T. C. (1987) Isotopic fractionation of nitrogen and carbon in the synthesis of amino acids by microorganisms. *Chem. Geol.: Isotope Geosci. Section* **65**, 79–92.
- McCarthy M. D., Lehman J. and Kudela R. (2013) Compound-specific amino acid δ<sup>15</sup>N patterns in marine algae: tracer potential for cyanobacterial vs. eukaryotic organic nitrogen sources in the ocean. *Geochim. Cosmochim. Acta* **103**, 104–120.
- McClelland J. W. and Montoya J. P. (2002) Trophic relationships and the nitrogen isotopic composition of amino acids in plankton. *Ecology* **83**, 2173–2180.
- McRose D. L., Baars O., Morel F. M. M. and Kraepiel A. M. L. (2017) Siderophore production in *Azotobacter vinelandii* in response to Fe-, Mo- and V-limitation. *Environ. Microbiol.* **48**, 11451–13605.
- Meador T. B., Aluwihare L. I. and Mahaffey C. (2007) Isotopic heterogeneity and cycling of organic nitrogen in the oligotrophic ocean. *Limnol. Oceanogr.* **52**, 934–947.
- Minagawa M. and Wada E. (1986) Nitrogen isotope ratios of red tide organisms in the East China Sea: A characterization of biological nitrogen fixation. *Mar. Chem.* **19**, 245–259.
- Montoya J. P. (2008) Nitrogen stable isotopes in marine environments. In *Nitrogen in the Marine Environment* (eds. D. G. Capone, D. A. Bronk, M. R. Mulholland and E. J. Carpenter), 2nd ed. Elsevier, pp. 1277–1302.
- Mulholland M. R., Bronk D. A. and Capone D. G. (2004) Dinitrogen fixation and release of ammonium and dissolved organic nitrogen by *Trichodesmium* IMS101. *Aquat. Microb. Ecol.* **37**, 85–94.
- Narula N., Lakshminarayana K. and Tauro P. (1981) Ammonia excretion by *Azotobacter chroococcum*. *Biotechnol. Bioeng.* **23**, 467–470.
- Narula N. and Gupta K. G. (1986) Ammonia excretion by *Azotobacter chroococcum* in liquid culture and soil in the presence of manganese and clay minerals. *Plant Soil* **93**, 205–209.
- Page W. J., Collinson S. K., Demange P., Dell A. and Abdallah M. A. (1991) *Azotobacter vinelandii* strains of disparate origin produce azotobactin siderophores with identical structures. *Biol. Met.* **4**, 217–222.
- Page W. J. and Sadoff H. L. (1976) Physiological factors affecting transformation of *Azotobacter vinelandii*. *J. Bacteriol.* **125**, 1080–1087.
- R Core Team (2012) *R: A Language and Environment for Statistical Computing*. R Foundation for Statistical Computing.
- Revillas J. J., Rodelas B., Pozo C., Martinez-Toledo M. V. and Gonzalez-Lopez J. (2000) Production of B-group vitamins by two *Azotobacter* strains with phenolic compounds as sole carbon source under diazotrophic and adiazotrophic conditions. *J. Appl. Microbiol.* **89**, 486–493.
- Robson, R.L., Eady, R.R., Richardson, T.H., Miller, R.W., Hawkins, M., Postgate, J.R., 1986. The alternative nitrogenase of *Azotobacter chroococcum* is a vanadium enzyme.
- Rowell, P., James, W., Smith, W.L., Handley, L.L., 1998. <sup>15</sup>N discrimination in molybdenum-and vanadium-grown N<sub>2</sub>-fixing

- Anabaena variabilis* and *Azotobacter vinelandii*. 30, pp. 2177–2180.
- Seefeldt L. C., Hoffman B. M. and Dean D. R. (2009) Mechanism of Mo-dependent nitrogenase. *Annu. Rev. Biochem.* **78**, 701–722.
- Sigman D. M., Casciotti K. L., Andreani M., Barford C., Galanter M. and Böhlke J. K. (2001) A bacterial method for the nitrogen isotopic analysis of nitrate in seawater and freshwater. *Anal. Chem.* **73**, 4145–4153.
- Sigman D., Karsh K. and Casciotti K. (2009a) *Ocean Process Tracers: Nitrogen Isotopes in the Ocean. Encyclopedia of Ocean Science*, 2nd edn. Elsevier, Amsterdam.
- Sigman D. M., DiFiore P. J., Hain M. P., Deutsch C., Wang Y., Karl D. M., Knapp A. N., Lehmann M. F. and Pantoja S. (2009b) The dual isotopes of deep nitrate as a constraint on the cycle and budget of oceanic fixed nitrogen. *Deep Sea Res. Part I: Oceanogr. Res. Papers* **56**, 1419–1439.
- Sim M. S., Ono S., Donovan K., Templer S. P. and Bosak T. (2011) Effect of electron donors on the fractionation of sulfur isotopes by a marine *Desulfovibrio* sp. *Geochim. Cosmochim. Acta* **75**, 4244–4259.
- Stüeken E. E., Buick R., Guy B. M. and Koehler M. C. (2015) Isotopic evidence for biological nitrogen fixation by molybdenum-nitrogenase from 3.2 Gyr. *Nature* **520**, 666–669.
- Tanabe T., Funahashi T., Nakao H., Miyoshi S. I., Shinoda S. and Yamamoto S. (2003) Identification and characterization of genes required for biosynthesis and transport of the siderophore vibrioferrin in *Vibrio parahaemolyticus*. *J. Bacteriol.* **185**, 6938–6949.
- Trick C. G. and Kerry A. (1992) Isolation and purification of siderophores produced by cyanobacteria, *Synechococcus* sp. PCC 7942 and *Anabaena variabilis* ATCC 29413. *Curr. Microbiol.* **24**, 241–245.
- Wada E. and Hattori A. (1976) Natural abundance of  $^{15}\text{N}$  in particulate organic matter in the North Pacific Ocean. *Geochim. Cosmochim. Acta* **40**, 249–251.
- Weigand M. A., Foriel J., Barnett B., Oleynik S. and Sigman D. M. (2016) Updates to instrumentation and protocols for isotopic analysis of nitrate by the denitrifier method. *Rapid Commun. Mass Spectrom.* **30**, 1365–1383.
- Yodsang P., Pothipongsa A., Mäenpää P. and Incharoensakdi A. (2014) Involvement of polyamine binding protein D (PotD) of *Synechocystis* sp. PCC 6803 in spermidine uptake and excretion. *Curr. Microbiol.* **69**, 417–422.
- Yoneyama F., Yamamoto M., Hashimoto W. and Murata K. (2011) *Azotobacter vinelandii* gene clusters for two types of peptidic and catechol siderophores produced in response to molybdenum. *J. Appl. Microbiol.* **111**, 932–938.
- Zerkle A. L., Junium C. K., Canfield D. E. and House C. H. (2008) Production of  $^{15}\text{N}$ -depleted biomass during cyanobacterial  $\text{N}_2$ -fixation at high Fe concentrations. *J. Geophys. Res. Biogeosci.* **113**, 535.
- Zerkle A. L., Poulton S. W., Newton R. J., Mettam C., Claire M. W., Bekker A. and Junium C. K. (2017) Onset of the aerobic nitrogen cycle during the Great Oxidation Event. *Nature* **542**, 465–467.
- Zhang X., Sigman D. M., Morel F. M. M. and Kraepiel A. M. L. (2014) Nitrogen isotope fractionation by alternative nitrogenases and past ocean anoxia. *PNAS* **111**, 4782–4787.

Associate editor: Jon Chorover